Dark biological superoxide production as a significant flux and sink of marine dissolved oxygen

Kevin M. Sutherland[a,b], Scott D. Wankel[a], and Colleen M. Hansel[a,1]

[a]Department of Marine Chemistry and Geochemistry, Woods Hole Oceanographic Institution, Woods Hole, MA 02543; and [b]Department of Earth, Atmospheric and Planetary Science, Massachusetts Institute of Technology, Cambridge, MA 02139

Edited by Donald E. Canfield, Institute of Biology and Nordic Center for Earth Evolution, University of Southern Denmark, Odense M., Denmark, and approved January 3, 2020 (received for review July 19, 2019)

The balance between sources and sinks of molecular oxygen in the oceans has greatly impacted the composition of Earth's atmosphere since the evolution of oxygenic photosynthesis, thereby exerting key influence on Earth's climate and the redox state of (sub)surface Earth. The canonical source and sink terms of the marine oxygen budget include photosynthesis, respiration, photorespiration, the Mehler reaction, and other smaller terms. However, recent advances in understanding cryptic oxygen cycling, namely the ubiquitous one-electron reduction of O_2 to superoxide by microorganisms outside the cell, remains unexplored as a potential player in global oxygen dynamics. Here we show that dark extracellular superoxide production by marine microbes represents a previously unconsidered global oxygen flux and sink comparable in magnitude to other key terms. We estimate that extracellular superoxide production represents a gross oxygen sink comprising about a third of marine gross oxygen production, and a net oxygen sink amounting to 15 to 50% of that. We further demonstrate that this total marine dark extracellular superoxide flux is consistent with concentrations of superoxide in marine environments. These findings underscore prolific marine sources of reactive oxygen species and a complex and dynamic oxygen cycle in which oxygen consumption and corresponding carbon oxidation are not necessarily confined to cell membranes or exclusively related to respiration. This revised model of the marine oxygen cycle will ultimately allow for greater reconciliation among estimates of primary production and respiration and a greater mechanistic understanding of redox cycling in the ocean.

microbial superoxide | reactive oxygen species | marine dissolved oxygen

Carbon fixation by oxygenic phototrophs produces O_2 in marine and terrestrial environments. On short timescales, the concentration of O_2 in the atmosphere and dissolved in the global ocean is maintained by an equal and opposite series of oxygen-consuming reactions. The preeminent of these O_2 loss terms is cellular respiration, although multiple additional loss processes are operative in oxygenic phototrophs (1–3). These include photorespiration, which occurs when the enzyme RuBisCO (ribulose-1,5-bisphosphate carboxylase/oxygenase) uses O_2 as a substrate instead of CO_2 in the reaction with ribulose 1,5-bisphosphate (RuBP) as part of the normal functioning of the Calvin–Benson–Bassham cycle. Loss of O_2 through photorespiration may be as high as 30% of gross oxygen production (GOP) (4, 5). The Mehler reaction is another significant oxygen loss term in oxygenic phototrophs, occurring when O_2 is reduced to superoxide ($O_2^{\bullet-}$) by electrons evolved from reduced ferredoxin in photosystem I in the presence of light (3). The fraction of O_2 evolved from photosystem II that is subsequently lost to reduction via the Mehler reaction is estimated at 10% of photosynthetically evolved O_2 in higher plants (5). These estimates of photosynthetic oxygen loss are based on model organisms of varying environmental relevance, and a great deal of uncertainty remains concerning how oxygen reduction in the environment is distributed among these many sinks. In algae, for example, O_2 photoreduction appears to be largely insensitive to dissolved inorganic carbon concentrations, even when the subject lacked a CO_2 concentrating mechanism (2). Studies of Mehler-related oxygen reduction in some cyanobacteria have been shown to exceed 40% of GOP (6, 7). Altogether, these studies demonstrate that Mehler-related oxygen loss in marine cyanobacteria and algae likely represents a larger proportion of total nonrespiratory O_2 reduction than is observed in higher plants.

The role of intracellular superoxide production as a significant sink of oxygen has been recognized since the 1950s for its place in the Mehler reaction (8); however, the role of extracellular superoxide production as an oxygen sink in both the presence and absence of light has not been assessed. Yet, dark (light-independent) particle-associated superoxide production accounts for a significant fraction of superoxide measured in natural waters within both the photic and aphotic zone (9, 10). Dark, extracellular superoxide production is in fact prolific among marine heterotrophic bacteria, cyanobacteria, and eukaryotes (9, 11–18). Production of extracellular superoxide proceeds via a one-electron transfer initiated by transmembrane, outer membrane-bound, or soluble extracellular enzymes thought to belong generally to NAD(P)H oxidoreductases (19), and more recently to heme peroxidases and glutathione reductases (9, 20, 21). At circumneutral pH, the superoxide anion ($O_2^{\bullet-}$) dominates over the conjugate acid $HO_2^{\bullet}$ ($pK_a = 4.8$) (22). This short-lived, reactive anion is highly impermeable to cell membranes (23). Thus, limited transmembrane diffusion and proportionally low levels of intracellular superoxide are insufficient to account for observed

Significance

Extracellular production of the reactive oxygen species (ROS) superoxide results from the one-electron reduction of O_2. Nearly all major groups of marine microbes produce extracellular superoxide. In this global estimate of marine microbial superoxide production we determine that dark extracellular superoxide production is ultimately a net sink of dissolved oxygen comparable in magnitude to other major terms in the marine oxygen cycle. This abundant source of superoxide to the marine water column provides evidence that extracellular ROS play a significant role in carbon oxidation and the redox cycling of metals in marine environments. Consideration of this significant reductive flux of dissolved oxygen is essential for field, laboratory, and modeling techniques for determining productivity and oxygen utilization in marine systems.

Author contributions: K.M.S., S.D.W., and C.M.H. designed research; K.M.S. performed research; K.M.S. analyzed data; and K.M.S., S.D.W., and C.M.H. wrote the paper.

The authors declare no competing interest.

This article is a PNAS Direct Submission.

[1]To whom correspondence may be addressed. Email: chansel@whoi.edu.

This article contains supporting information online at https://www.pnas.org/lookup/suppl/doi:10.1073/pnas.1912313117/-/DCSupplemental.

extracellular fluxes (9, 23, 24). Superoxide has a half-life on the order of a few minutes or less (9, 25), with its fate highly dependent on seawater chemistry; superoxide may be reoxidized to O_2 or reduced to H_2O_2, other peroxides, and ultimately water by reactions with redox-active metals including copper, iron, and manganese, organic matter, or via (un)catalyzed dismutation (26, 27).

Extracellular superoxide plays a diverse suite of roles in cell physiology, including cell signaling, growth, defense, and redox homeostasis. In microbial eukaryotes, enzymatic extracellular superoxide production is involved in cell differentiation (19). In plants, superoxide serves as a pretranscription defense in wound repair (16). Recently, extracellular superoxide within marine bacteria was shown to be tightly regulated through the growth cycle with superoxide eliminated upon entering stationary phase (28). Addition of superoxide dismutase (SOD), an enzyme that eliminates superoxide, inhibited growth, suggesting that superoxide is involved in growth and proliferation as previously suggested for pathogenic strains of *Escherichia coli* and *Chattonella marina* (29–32). Further, recent evidence indicates that extracellular superoxide production by the diatom *Thalassiosira oceanica* may play a critical role in maintaining the internal redox conditions in photosynthesizing cells (21). This suite of beneficial physiological processes all result from or result in the reduction of molecular oxygen that is not otherwise considered in biogeochemical cycles of oxygen and related elements.

Our aim in this study is to leverage recent assessments of dark extracellular superoxide production rates by globally important groups of marine microbes to determine the resulting oxygen sink. Our approach consists of two parts: 1) constrain the gross oxygen reduction that results from dark, extracellular superoxide production and 2) estimate the fraction of gross superoxide produced that is ultimately reduced to water. Generally speaking, the most abundant group of organisms in the global ocean is heterotrophic bacteria. Alphaproteobacteria and Gammaproteobacteria comprise >70% of heterotrophic bacteria in the water column, and a subset of Alphaproteobacteria, Pelagibacterales (SAR11 clade), makes up nearly 25% of cells in the ocean (33, 34). Here we compile measured extracellular superoxide production rates of several marine Alphaproteobacteria and Gammaproteobacteria, including SAR11 clade organisms (Fig. 1). Although far outnumbered by marine heterotrophs in the global ocean, oxygenic phototrophs have been shown to produce both light-dependent and -independent extracellular superoxide up to several orders of magnitude higher than average marine heterotrophs on a per-cell basis, meaning a representative accounting of the superoxide flux from phototrophs is necessary to adequately constrain superoxide production (9, 13, 35). In this study we include superoxide production rates of the following organisms: *Prochlorococcus* and *Synechococcus*, the two most abundant photosynthetic organisms in the global ocean; *Trichodesmium*, a dominant N_2-fixing cyanobacterium in oligotrophic waters; coccolithophores, the most abundant group of calcifying microalgae present throughout the global ocean; several species of diatoms, a diverse group of silicifying algae found in nutrient rich waters; and *Phaeocystis*, an alga predominately found in the Southern Ocean. In constructing this estimate of superoxide production, we assign measured dark superoxide production rates to organisms that fall within these groups of organisms and conservatively consider all others to be nonproducing.

Marine heterotrophs belonging to Alphaproteobacteria and Gammaproteobacteria, including two Pelagibacterales members, produce gross extracellular superoxide within a fairly narrow range of 0.1 to 3.7 amol·cell^{-1}·h^{-1} (Fig. 1). Oxygenic phototrophs, with the exception of *Prochlorococcus*, far exceed heterotrophic cell-normalized superoxide production, with net production rates ranging from 4.3 to 13,400 amol·cell^{-1}·h^{-1} (17). *Prochlorococcus* produces significantly less extracellular superoxide across four ecotypes, with average gross rates ranging from 0.007 to 0.091 amol·cell^{-1}·h^{-1} (17).

Also shown in Fig. 1 is an estimate for the average marine cell O_2 utilization rate assuming a balanced marine oxygen budget (see *SI Appendix* for calculation), or in other words the total amount of oxygen produced in the global ocean, divided by the number of cells. This estimate demonstrates that dark extracellular superoxide production of several groups of marine organisms exceeds the average oxygen utilization rate. Here we use the more general term "oxygen utilization" instead of "respiration" because other oxygen-consuming biological reactions (e.g., photorespiration

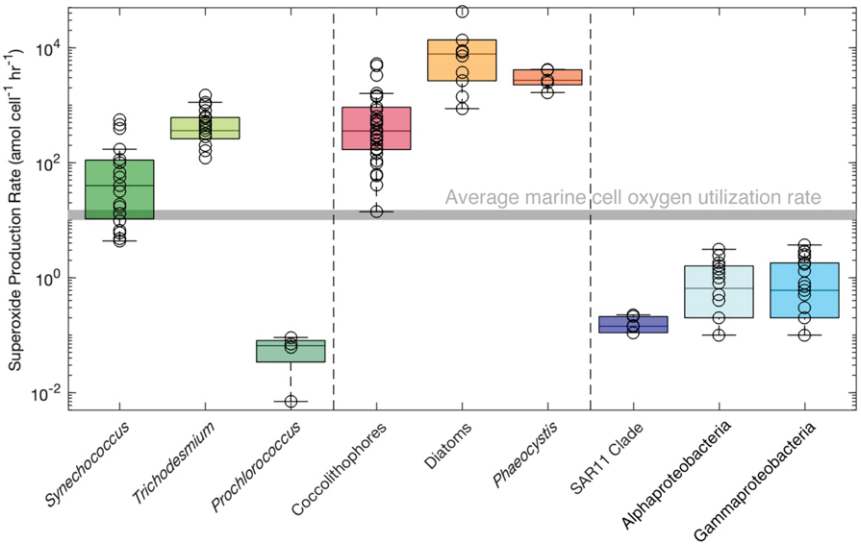

Fig. 1. Extracellular superoxide production rates. Cyanobacteria (green) include *Synechococcus*, *Trichodesmium*, and *Prochlorococcus*; eukaryotic algae (orange) include coccolithophores, diatoms, and *Phaeocystis*; and heterotrophic bacteria (blue) include Pelagibacterales (SAR11 clade), other Alphaproteobacteria, and Gammaproteobacteria (see *SI Appendix* for data, sources, and organism details and *SI Appendix*, Table S1 for diatom rates). Average marine cell oxygen consumption rate is shown in gray (*SI Appendix*).

Table 1. Estimate of global superoxide flux: Summary of cell number estimates, cell specific superoxide production rates, and contribution of each marine clade toward the marine superoxide flux

Group	Cell estimate*	Range superoxide production, amol·cell^{-1}·h^{-1}	Mean model value*, amol·cell^{-1}·h^{-1}	Superoxide production, mol·y^{-1}
Synechococcus	7.0×10^{26}	4.3–550	106	6.49×10^{14}
Trichodesmium	4.6×10^{23}	ND-1,500	465	1.87×10^{12}
Prochlorococcus	2.9×10^{27}	0.007–0.091	0.06	1.40×10^{12}
Coccolithophores	2.6×10^{26}	ND-5,300	342	7.78×10^{14}
Diatoms	2.6×10^{24}	75–13,000	47,560†	1.07×10^{15}
Phaeocystis	3.9×10^{25}	1,700–4,200	2,925	9.99×10^{14}
Pelagibacterales (SAR11)	2.4×10^{28}	0.11–0.23	0.15	3.20×10^{13}
Alphaproteobacteria (without SAR11)	1.9×10^{28}	0.1–3.1	0.9	1.51×10^{14}
Gammaproteobacteria	2.7×10^{28}	0.1–3.7	1.1	2.57×10^{14}
Total				3.94×10^{15}

ND = measurement reported below method detection limit.
*See *SI Appendix* for sources, derivations of cell number estimates, and model value assignment.
†Calculated using cell surface area normalized rates; see *SI Appendix*.

and the Mehler reaction) are each responsible for >10% of the marine oxygen sink. To extrapolate these superoxide production values to the global ocean, we provide estimates of total cell numbers in the water column of each organismal group included in this study (Table 1). We assigned cells from each group the mean and standard error (SE) determined from our bootstrapping approach and used a Monte Carlo approach to determine the mean and probability distribution for the whole ocean superoxide flux. A slightly different approach was used for diatoms (*Methods*). Using these total cell number estimates and modeled dark extracellular superoxide production rates for each organismal group, we calculate that gross dark extracellular superoxide production represents a flux of 3.9 (± 0.5) × 10^{15} mol O_2 per year. For comparison, a central estimate for GOP in all marine environments derived from estimates of marine productivity is 1.09 × 10^{16} mol O_2 y^{-1} (*SI Appendix*) (36). Thus, gross light-independent extracellular superoxide production by microorganisms represents an O_2 loss flux ~36 (± 5)% of marine GOP. This gross superoxide production estimate is illustrative for demonstrating the size of this reductive flux; however, it is the net reduction of superoxide that ultimately determines the weight of this reductive flux on the global oxygen cycle. We provide constraints on the net reduction of extracellular superoxide below.

While we show that model estimates based on laboratory-based rates yield a dark superoxide flux that is a substantial and previously unrecognized part of the global oxygen budget, a claim that represents such a significant shift in the model of marine oxygen utilization requires some ground truthing with environmental data. In particular, we used a bootstrapping approach to estimate the mean and SE of all extracellular superoxide production rates available in the literature for each group discussed here (*SI Appendix*, Fig. S1). The available data on extracellular superoxide production within axenic cultures do not contain the ideal richness for relying on this numerical approach alone. Thus, we tested our culture-based estimate by calculating expected marine superoxide concentrations based on our estimate of global superoxide production and compared these values to available marine superoxide concentration data. If our estimate for average marine superoxide concentration falls within observations, this provides an independent line of evidence that extracellular superoxide production comprises a significant global oxygen flux, with our reasoning as follows. The mean pseudo-first-order decay rate constant of superoxide in marine environments has been previously characterized at 0.0106 s^{-1}, with a 1σ confidence interval from 0.0050 s^{-1} to 0.0226 s^{-1} (*SI Appendix*, Fig. S3) (35, 37–39). Using these observed decay rate constants we estimate steady-state superoxide concentrations from biological production to be 152 pM (1σ confidence interval: 71 to 322 pM) in the surface ocean and 0.6 pM (1σ confidence interval: 0.3 to 1.3 pM) below 200 m (*SI Appendix*, Table S2). All available superoxide concentration measurements from the marine water column are shown in Fig. 2 along with the calculated expected concentration range based on our model of global superoxide production (gray bar). As indicated, the expected range of superoxide concentrations is largely consistent with measurements collected in the surface ocean, and, in fact, underestimates measured concentrations in all deep ocean measurements. Although not shown in Fig. 2, superoxide concentrations in some coastal systems

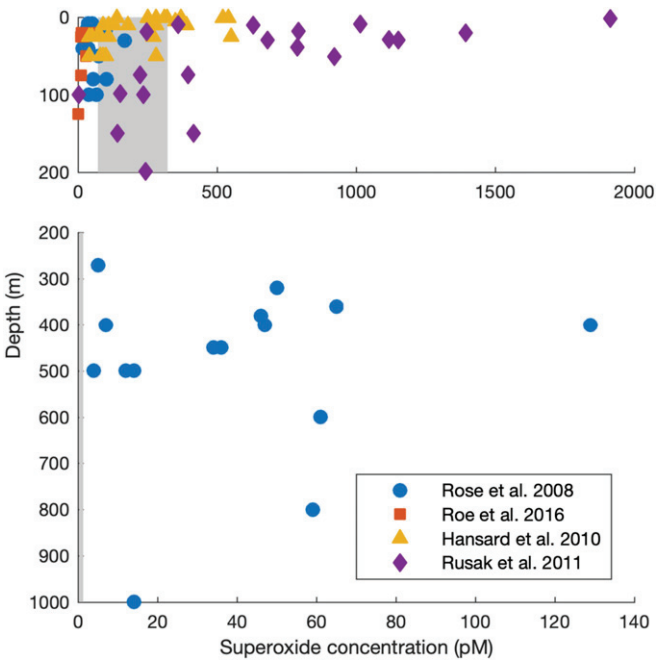

Fig. 2. Measured and expected marine superoxide concentration. Compiled marine superoxide measurements from Rose et al. (35) (green diamond), Hansard et al. (38) (yellow triangle), Rusak et al. (39) (red square), and Roe et al. (37) (blue circle). The gray bars indicate the 68% confidence interval for the expected superoxide concentration based on our total superoxide flux estimate. The 68% confidence intervals for the expected superoxide concentrations in the surface (<200 m) and deep (>200 m) ocean are 71 to 322 pM and 0.3 to 1.3 pM, respectively.

have been reported as high as 120 nM, four orders of magnitude higher than our estimate, underscoring the conservative nature of our estimate (40).

Additional Sources of Superoxide

This accounting of the marine superoxide flux only considers extracellular dark superoxide production by dominant organisms with known production rates. In fact, the total O_2 flux via all superoxide production pathways in marine environments undoubtedly exceeds our estimates here by a sizable margin and would lead to an even greater contribution of superoxide production on O_2 loss. In particular, light-dependent (a)biotic superoxide production is not included in our present estimate. Within sunlit waters, there is significant abiotic photochemical production of superoxide, and extracellular superoxide production rates by marine phototrophs are significantly higher in the light (13, 41, 42). Indeed, the extracellular superoxide production exhibited by multiple species of diatoms more than doubled in the presence of light (42). The same behavior was observed for the coccolithophore *Emiliania Huxleyi* (18) and certain *Trichodesmium* ecotypes (13), where light-dependent increases in extracellular superoxide could not be accounted for by abiotic factors. Since phototrophs as a group are responsible for most of the dark extracellular superoxide production, even modest modulation in extracellular superoxide production in the light could produce a substantial increase in our estimate of the gross superoxide flux and the net oxygen sink that results, which we discuss in the next section.

Possibly the best-characterized abiotic source of superoxide in the oceans is the photochemical excitation of chromophoric dissolved organic matter (CDOM) and subsequent reduction of O_2 to superoxide in the surface ocean (43). One model using a remote sensing approach to estimate photochemical reactive oxygen species (ROS) production in the surface ocean estimated that midday superoxide concentrations resulting from photochemical production and a range of superoxide sinks ranged from near 10 pM at high latitudes to near 200 pM at low latitudes (41). These results demonstrate that photochemical production of superoxide can exceed dark biological production in sunlit surface waters. Notably, contribution of this photochemical superoxide will vary temporally and decrease with depth upon the attenuation of photoactive wavelengths (290 to 490 nm), with local variations in productivity and the compositional nature of surface ocean CDOM also impacting its reactivity.

The Fate of Superoxide

Both laboratory- and field-based measurements converge on the similar conclusion that dark extracellular superoxide flux is a substantial component of oxygen turnover in the global ocean. To further place this process into the context of the global O_2 budget, it is important to distinguish gross dark superoxide production from the net loss of dissolved O_2. Superoxide in aqueous systems may decay by oxidation back to O_2, with no net effect on marine dissolved oxygen, or via reduction, which may lead to a net loss of oxygen. Superoxide decay is considered the primary source of hydrogen peroxide (H_2O_2), and thus much of what we know and assume about the fate of superoxide is inferred from studies of hydrogen peroxide concentration and rate measurements. Nevertheless, other secondary and direct sources of hydrogen peroxide have also been identified within microbial cultures (42, 44, 45) and natural waters (10). For the purposes of this estimate, we accept the general premise that superoxide decay is the primary source of hydrogen peroxide and ignore other sources, while recognizing that the foundation of this premise needs further evaluation. It is also often assumed that the primary reduction or disproportionation product of superoxide production is H_2O_2; however, superoxide decay may also occur through bond-forming redox reactions with dissolved organic carbon, metals, or through unknown sinks (46–50). Such reactions will not produce an H_2O_2 intermediate. In fact, it has been shown that hydrogen peroxide formation can only account for 45% of net oxygen loss in photochemical oxidation of marine waters (50). While photochemical superoxide production is not a perfect analogy for dark biological superoxide production, the large body of work investigating the fate of photochemically derived superoxide offers the most transferable insight into the likely fate of biologically derived superoxide in seawater. What follows is our attempt to constrain the net reduction of marine dissolved oxygen from the estimate of gross extracellular superoxide production using a combination of measurements from photochemical and biogeochemical literature.

Ultimately, the fate of superoxide and hydrogen peroxide is highly dependent on the availability of dissolved organic matter (and its reactivity), the abundance of redox-active metals (and their redox states), and the expression of enzymes that eliminate ROS such as SOD, catalase, and peroxidases (49, 51, 52). Superoxide can be both oxidized (Eq. **1**) and reduced (Eq. **2**), leading to the net consumption of 0 or 1 mol O_2 per mole superoxide, respectively (Fig. 3). Superoxide can also undergo uncatalyzed dismutation, a process that results in 50% oxidation to O_2 and 50% reduction to H_2O_2 (Eq. **3**). Hydrogen peroxide is more stable than superoxide in natural waters, with pseudo-first-order decay rate constants approximately three orders of magnitude lower than that of superoxide. Consequently, H_2O_2 has a lifetime of ~1 to 2 d, and typical concentrations are $\sim 10^3$ higher for H_2O_2 than for superoxide [from <1 nM in the deep ocean to ~100 nM in sunlight surface water (53, 54)]. Typical production and decay rates range from 0.8 to 2.4 $nM \cdot h^{-1}$ for dark seawater (53) and 0.9 to 8.3 $nM \cdot h^{-1}$ in sunlit seawater (55). As for the fate of H_2O_2, previous work has shown that light-independent, biological processes are primarily responsible for its degradation in marine systems, with 65 to 80% of H_2O_2 degradation resulting from catalase activity (Eq. **4**) and the remainder resulting from peroxidase activity (Eq. **5**) (53):

$$O_2^{\cdot-} \rightarrow O_2 + e^- \left(O_2^{\cdot-}\text{oxidation}\right) \quad [1]$$

$$O_2^{\cdot-} + 2H^+ + e^- \rightarrow H_2O_2 \left(O_2^{\cdot-}\text{reduction}\right) \quad [2]$$

$$2O_2^{\cdot-} + 2H^+ \rightarrow H_2O_2 + O_2 (\text{SOD or uncatalyzed dismutation}) \quad [3]$$

$$2H_2O_2 \rightarrow 2H_2O + O_2 (\text{catalase-based } H_2O_2 \text{ decay}) \quad [4]$$

$$H_2O_2 + AH_2 \rightarrow 2H_2O + A (\text{peroxidase-based } H_2O_2 \text{ decay}). \quad [5]$$

Assuming this range of catalase and peroxidase activity holds throughout the water column, between 60 and 67.5% of H_2O_2 is

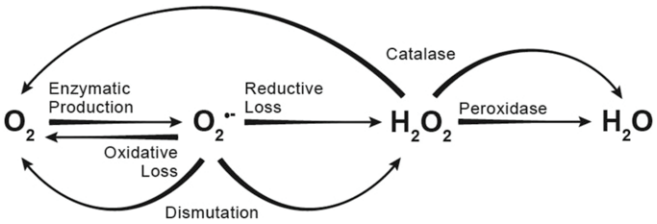

Fig. 3. Decay pathways of superoxide in biogeochemical systems. Summary of superoxide decay pathways in marine environments. Superoxide, once produced, may be oxidized to O_2 and/or reduced to H_2O_2 (or other peroxides). Peroxides may be oxidized to O_2 and/or reduced to H_2O. The net dissolved oxygen sink that results from extracellular superoxide production is the product of gross production and that fraction of O_2 that is ultimately reduced to water.

ultimately reduced to water. Thus, the theoretical net loss of oxygen through the superoxide production pathway can range from 0 (e.g., all superoxide is oxidized back to O_2; Eq. **1**) to 67.5% (e.g., superoxide reduction to H_2O_2; Eq. **2**), followed by catalase- and peroxidase-mediated degradation of H_2O_2 (Eqs. **4** and **5**) (Fig. 3).

There are two ways we can use previous data to estimate the net sink of oxygen that results from the dark biological superoxide flux in the ocean. The first, and more conservative, approach is to multiply the global superoxide production flux by the ratio of hydrogen peroxide production to superoxide production observed in natural waters, P_{H2O2}/P_{O2-}, followed by the oxidation–reduction ratio observed for hydrogen peroxide. This yields the total O_2 reduced to water via an H_2O_2 intermediate and accounts for dismutation (Eq. **3**), univalent oxidation (Eq. **1**), and univalent reduction (Eq. **2**). This method will produce a more conservative estimate of net oxygen loss because it implicitly assumes that all superoxide not reduced to hydrogen peroxide is reoxidized to O_2, when in reality a large fraction of the superoxide sink may yield products other than hydrogen peroxide (e.g., organic peroxides or other ROS) (49, 50). The second approach uses the same P_{H2O2}/P_{O2-} ratio to determine the hydrogen peroxide flux that results from the superoxide flux, multiplied by the observed ratio of net oxygen loss to hydrogen peroxide formation in a marine photochemical system where superoxide is implicated as the primary oxidant. This approach may slightly overestimate the net oxygen sink because it ignores the possibility that some oxygen reduction may occur through multielectron transfers (50).

For both of these approaches, we need a reasonable estimate of the production ratio of hydrogen peroxide to that of superoxide (P_{H2O2}/P_{O2-}). In experiments investigating production of superoxide and hydrogen peroxide during DOM irradiation, P_{H2O2}/P_{O2-} ranged from 0.10 to 0.67, with an average value of 0.24 (55). Another similar study on waters collected from the transition between terrestrial and marine environment found that P_{H2O2}/P_{O2-} ranged from ∼0.5 in riverine waters to ∼0.30 in Gulf Stream waters (56). Slightly lower values (0.08 to 0.17) have been observed in photochemical systems with terrestrial organic matter (57), possibly due to the differing nature of terrestrial DOM (aromatic vs. aliphatic). In a brackish and a freshwater pond, P_{H2O2}/P_{O2-} sometimes exceeded the stoichiometry of 0.5 expected for dismutation, suggesting there may be other sources of hydrogen peroxide (10). We use the average value presented by Powers et al. (55) of 0.24 as the most relevant to the marine environment and the best choice at this time for a global marine estimate. Using our first approach and P_{H2O2}/P_{O2} of 0.24, we estimate a lower bound for the net oxygen reduction resulting from superoxide production at 14.4% of the marine superoxide flux (or 5% of the marine oxygen budget). A significant fraction of this superoxide (52% of the marine superoxide flux) is unaccounted for because it does not produce hydrogen peroxide, meaning the fate of as much as 19% of the marine oxygen budget that cycles through superoxide remains unknown.

Using the second approach, we assume hydrogen peroxide formation and net oxygen loss that result from superoxide formation occur with a fixed ratio in seawater [0.45:1 H_2O_2:$-O_2$ (50)]. We find that superoxide production will result in a net oxygen loss of 53% of the global superoxide flux (or 19% of the marine oxygen budget).

These two estimation methods suggest dark, biological production of extracellular superoxide is a sink between 5 and 19% in the marine oxygen budget, indicating that the oxygen sink from dark extracellular superoxide production is similar in magnitude to the Mehler reaction and photorespiration. Notably, total superoxide production in photochemical systems has been shown to correlate with CO_2 production from DOM (58), suggesting that a significant fraction of the superoxide sink is ultimately through reduction tied to organic carbon oxidation, favoring the higher end of this estimate. Shipboard incubations show that marine superoxide decay is primarily correlated with dissolved organic matter and dissolved manganese, both of which allow for a significant reductive sink of superoxide (26, 51) and subsequent higher O_2 loss. Oxygen loss in marine environments has previously been attributed primarily to a combination of respiration, photorespiration, and the Mehler reaction in the surface ocean and respiration alone in the deep ocean. We propose that dark extracellular superoxide production and its net oxygen sink has likely been overlooked and unintentionally incorporated into other sinks because separation of this secondary physiological process presents a methodological challenge. The sinks of marine oxygen resulting from respiration, photorespiration, and the Mehler reaction should therefore be revised downward to accommodate for the reductive sink from extracellular superoxide production.

Further Implications

We anticipate that the identification of an appreciable cryptic sink of oxygen, and consequently organic carbon, may help reconcile spatiotemporal and methodological discrepancies among measurements of marine primary productivity arising as variable contributions of superoxide production to net O_2 loss. Adding another layer of complexity, the resulting H_2O_2 produced in excess during times of increased metabolic activity (e.g., photosynthetic organisms under full light) may store oxidizing equivalents that persist in the environment for hours to days. These processes may lead to heterogeneous O:C reaction stoichiometry as well as possible complexity in corresponding stable isotope dynamics. As measurements of primary productivity collected using multiple methods concurrently can produce primary productivity estimates that vary more than an order of magnitude (59), we propose that cryptic ROS cycling and ROS-related oxygen loss may explain some of these discrepancies (e.g., ^{14}C vs. triple oxygen isotopes). Studies of respiration, respiration stoichiometries ($-O_2$:C), and respiration isotope effects will also be impacted if organism-level extracellular superoxide production rate is an appreciable fraction of respiration rate. The $-O_2$:C ratio of oxygen utilization in the water column has been observed to vary by up to 30% across different locations and ocean depths (60–62). Production of extracellular superoxide (coupled with the oxidation of intracellular reducing equivalents) may lead to differential redox evolution of marine carbon reservoirs that are spatially or functionally separated (e.g., surface vs. deep, particulate vs. dissolved). While superoxide production will not affect the whole ocean $-O_2$:C, it may drastically influence the amount and rate of organic carbon that is directly remineralized to CO_2 vs. that which proceeds through partially oxidized dissolved organic compounds. The exact utility of extracellular superoxide for cells and the magnitude of influence superoxide has on the global carbon budget (today and throughout Earth history) both remain important and open questions. Nevertheless, this newly identified gross flux of superoxide in the global ocean underscores the critical role ROS play in the global cycling of O_2, carbon, and redox active elements essential to life.

Methods

The dark superoxide production rates compiled in this study, with the exception of coccolithophores, were measured from cells grown to mid-exponential phase under ideal growth conditions using a flow-injection chemiluminescent approach (9). The study investigating the cell-specific superoxide production rate of coccolithophores measured their production rate throughout their growth curve, which we converted to a time-weighted average using trapezoidal integration of the cell superoxide production rate as a function of time (18). Cell-normalized superoxide production rates presented in the scientific literature are either presented as net or gross superoxide production rates, the latter requiring an exogenous spike of superoxide to determine the proportion of extracellular ROS that is enzymatically degraded by the organisms. Gross superoxide production rates

were used here when available; otherwise, net superoxide production rates were used. All compiled rates are presented in Fig. 1. Bootstrap resampling of extracellular superoxide production rates was conducted to estimate the rate distribution of each organism group (*SI Appendix*, Fig. S1), with the exception of diatoms. Diatom production rate was normalized to cell surface area and diatom surface area was determined from a database containing >90,000 georeferenced diatom observations (*SI Appendix*, Table S1). Cell abundances for phototroph and heterotroph groups included in this study were compiled or calculated from available literature data and are discussed in greater detail in *SI Appendix*. We note that when net primary productivity (NPP) estimates were used to estimate cell abundances, each group's fractional contribution to NPP (as opposed to moles of carbon fixed) was given preference. Fraction contribution to NPP was preferred because it allows for direct comparison between GOP and total superoxide production in a way that minimizes the influence of differences in productivity estimates between studies. Total superoxide flux was estimated using a Monte Carlo approach incorporating superoxide production rate distribution for each organism group. Parameter choices and results are presented in *SI Appendix, Estimation of Global Superoxide Flux*. Superoxide concentrations and uncertainties were estimated using the volume-normalized superoxide flux and a compilation of superoxide decay rates from the literature (*SI Appendix*, Fig. S3 and Table S2). Further experimental methods are described in *SI Appendix*. All data compiled and generated in this study are provided within the main text and *SI Appendix*.

ACKNOWLEDGMENTS. This work was supported by NASA Earth and Space Science Fellowship NNX15AR62H to K.M.S., NASA Exobiology grant NNX15AM04G to S.D.W. and C.M.H., and NSF Division of Ocean Sciences grant 1355720 to C.M.H. This research was further supported in part by Hanse-Wissenschaftskolleg Institute of Advanced Study fellowships to C.M.H. and S.D.W. We thank Danielle Hicks for assistance with figures and Community Earth Systems Model (CESM) Large Ensemble Project for the availability and use of its data product. The CESM project is primarily supported by the NSF.

1. M. Eisenhut *et al*., The photorespiratory glycolate metabolism is essential for cyanobacteria and might have been conveyed endosymbiontically to plants. *Proc. Natl. Acad. Sci. U.S.A.* **105**, 17199–17204 (2008).
2. M. R. Badger, S. von Caemmerer, S. Ruuska, H. Nakano, Electron flow to oxygen in higher plants and algae: Rates and control of direct photoreduction (Mehler reaction) and rubisco oxygenase. *Philos. Trans. R Soc. B-Biological Sci.* **355**, 1433–1445 (2000).
3. K. Asada, Production and scavenging of reactive oxygen species in chloroplasts and their functions. *Plant Physiol.* **141**, 391–396 (2006).
4. M. Bender, T. Sowers, L. Labeyrie, The Dole effect and its variations during the last 130,000 years as measured in the vostok ice core. *Global Biogeochem. Cycles* **8**, 363–376 (1994).
5. R. D. Guy, M. L. Fogel, J. A. Berry, Photosynthetic fractionation of the stable isotopes of oxygen and carbon. *Plant Physiol.* **101**, 37–47 (1993).
6. T. M. Kana, Rapid oxygen cycling in Trichodesmium thiebautii. *Limnol. Oceanogr.* **38**, 18–24 (1993).
7. Y. Helman, E. Barkan, D. Eisenstadt, B. Luz, A. Kaplan, Fractionation of the three stable oxygen isotopes by oxygen-producing and oxygen-consuming reactions in photosynthetic organisms. *Plant Physiol.* **138**, 2292–2298 (2005).
8. A. H. Mehler, Studies on reactions of illuminated chloroplasts. I. Mechanism of the reduction of oxygen and other Hill reagents. *Arch. Biochem. Biophys.* **33**, 65–77 (1951).
9. J. M. Diaz *et al*., Widespread production of extracellular superoxide by heterotrophic bacteria. *Science* **340**, 1223–1226 (2013).
10. T. Zhang, C. M. Hansel, B. M. Voelker, C. H. Lamborg, Extensive dark biological production of reactive oxygen species in brackish and freshwater ponds. *Environ. Sci. Technol.* **50**, 2983–2993 (2016).
11. C. M. Hansel, C. A. Zeiner, C. M. Santelli, S. M. Webb, Mn(II) oxidation by an ascomycete fungus is linked to superoxide production during asexual reproduction. *Proc. Natl. Acad. Sci. U.S.A.* **109**, 12621–12625 (2012).
12. D. R. Learman, B. M. Voelker, A. I. Vazquez-Rodriguez, C. M. Hansel, Formation of manganese oxides by bacterially generated superoxide. *Nat. Geosci.* **4**, 95–98 (2011).
13. C. M. Hansel *et al*., Dynamics of extracellular superoxide production by Trichodesmium colonies from the Sargasso Sea. *Limnol. Oceanogr.* **61**, 1188–1200 (2016).
14. A. B. Kustka, Y. Shaked, A. J. Milligan, D. W. King, F. M. M. Morel, Extracellular production of superoxide by marine diatoms: Contrasting effects on iron redox chemistry and bioavailability. *Limnol. Oceanogr.* **50**, 1172–1180 (2005).
15. D. Kim *et al*., Mechanism of superoxide anion generation in the toxic red tide phytoplankton Chattonella marina: Possible involvement of NAD(P)H oxidase. *Biochim. Biophys. Acta* **1524**, 220–227 (2000).
16. C. Lamb, R. A. Dixon, The oxidative burst in plant disease resistance. *Annu. Rev. Plant Physiol. Plant Mol. Biol.* **48**, 251–275 (1997).
17. K. M. Sutherland *et al*., Extracellular superoxide production by key microbes in the global ocean. *Limnol. Oceanogr.* **64**, 2679–2693 (2019).
18. S. Plummer, A. E. Taylor, E. L. Harvey, C. M. Hansel, J. M. Diaz, Dynamic regulation of extracellular superoxide production by the coccolithophore Emiliania huxleyi (CCMP 374). *Front. Microbiol.* **10**, 1546 (2019).
19. J. Aguirre, M. Ríos-Momberg, D. Hewitt, W. Hansberg, Reactive oxygen species and development in microbial eukaryotes. *Trends Microbiol.* **13**, 111–118 (2005).
20. P. F. Andeer, D. R. Learman, M. McIlvin, J. A. Dunn, C. M. Hansel, Extracellular haem peroxidases mediate Mn(II) oxidation in a marine Roseobacter bacterium via superoxide production. *Environ. Microbiol.* **17**, 3925–3936 (2015).
21. J. M. Diaz *et al*., NADPH-dependent extracellular superoxide production is vital to photophysiology in the marine diatom Thalassiosira oceanica. *Proc. Natl. Acad. Sci. U. S. A.* **116**, 16448–16453 (2019).
22. B. H. J. Bielski, D. E. Cabelli, R. L. Arudi, A. B. Ross, Reactivity of HO_2/O^-_2 radicals in aqueous solution. *J. Phys. Chem. Ref. Data* **14**, 1041–1100 (1985).
23. R. M. Cordeiro, Reactive oxygen species at phospholipid bilayers: Distribution, mobility and permeation. *Biochim. Biophys. Acta* **1838**, 438–444 (2014).
24. R. A. Gus'kova, I. I. Ivanov, V. K. Kol'tover, V. V. Akhobadze, A. B. Rubin, Permeability of bilayer lipid membranes for superoxide (O2−•) radicals. *Biochim. Biophys. Acta (BBA)-Biomembranes* **778**, 579–585 (1984).
25. M. A. Takahashi, K. Asada, Superoxide anion permeability of phospholipid membranes and chloroplast thylakoids. *Arch. Biochem. Biophys.* **226**, 558–566 (1983).
26. M. I. Heller, P. L. Croot, Kinetics of superoxide reactions with dissolved organic matter in tropical Atlantic surface waters near Cape Verde (TENATSO). *J. Geophys. Res.* **115**, C12038 (2010).
27. K. Wuttig, M. I. Heller, P. L. Croot, Reactivity of inorganic Mn and Mn desferrioxamine B with O2, O2(-), and H2O2 in seawater. *Environ. Sci. Technol.* **47**, 10257–10265 (2013).
28. C. M. Hansel, J. M. Diaz, S. Plummer, Tight regulation of extracellular superoxide points to its vital role in the physiology of the globally relevant Roseobacter clade. *mBio* **10**, e02668-18 (2019).
29. T. M. Buetler, A. Krauskopf, U. T. Ruegg, Role of superoxide as a signaling molecule. *News Physiol. Sci.* **19**, 120–123 (2004).
30. M. Saran, To what end does nature produce superoxide? NADPH oxidase as an autocrine modifier of membrane phospholipids generating paracrine lipid messengers. *Free Radic. Res.* **37**, 1045–1059 (2003).
31. A. Carlioz, D. Touati, Isolation of superoxide dismutase mutants in Escherichia coli: Is superoxide dismutase necessary for aerobic life? *EMBO J.* **5**, 623–630 (1986).
32. T. Oda *et al*., Catalase-and superoxide dismutase-induced morphological changes and growth inhibition in the red tide phytoplankton Chattonella marina. *Biosci. Biotechnol. Biochem.* **59**, 2044–2048 (1995).
33. L. Zinger *et al*., Global patterns of bacterial beta-diversity in seafloor and seawater ecosystems. *PLoS One* **6**, e24570 (2011).
34. S. J. Giovannoni, SAR11 bacteria: The most abundant plankton in the oceans. *Ann. Rev. Mar. Sci.* **9**, 231–255 (2017).
35. A. L. Rose, E. A. Webb, T. D. Waite, J. W. Moffett, Measurement and implications of nonphotochemically generated superoxide in the equatorial Pacific Ocean. *Environ. Sci. Technol.* **42**, 2387–2393 (2008).
36. C. B. Field, M. J. Behrenfeld, J. T. Randerson, P. Falkowski, Primary production of the biosphere: Integrating terrestrial and oceanic components. *Science* **281**, 237–240 (1998).
37. K. L. Roe, R. J. Schneider, C. M. Hansel, B. M. Voelker, Measurement of dark, particle-generated superoxide and hydrogen peroxide production and decay in the subtropical and temperate North Pacific Ocean. *Deep Res. Part I-Oceanogr. Res. Pap.* **107**, 59–69 (2016).
38. S. P. Hansard, A. W. Vermilyea, B. M. Voelker, Measurements of superoxide radical concentration and decay kinetics in the Gulf of Alaska. *Deep Sea Res. Part I* **57**, 1111–1119 (2010).
39. S. A. Rusak, B. M. Peake, L. E. Richard, S. D. Nodder, W. J. Cooper, Distributions of hydrogen peroxide and superoxide in seawater east of New Zealand. *Mar. Chem.* **127**, 155–169 (2011).
40. J. M. Diaz *et al*., Species-specific control of external superoxide levels by the coral holobiont during a natural bleaching event. *Nat. Commun.* **7**, 13801 (2016).
41. L. C. Powers, W. L. Miller, Blending remote sensing data products to estimate photochemical production of hydrogen peroxide and superoxide in the surface ocean. *Environ. Sci. Process. Impacts* **16**, 792–806 (2014).
42. R. J. Schneider, K. L. Roe, C. M. Hansel, B. M. Voelker, Species-level variability in extracellular production rates of reactive oxygen species by diatoms. *Front Chem.* **4**, 5 (2016).
43. J. V. Goldstone, B. M. Voelker, Chemistry of superoxide radical in seawater. CDOM associated sink of superoxide in coastal waters. *Environ. Sci. Technol.* **34**, 1043–1048 (2000).
44. B. Palenik, F. M. M. Morel, Amine oxidases of marine phytoplankton. *Appl. Environ. Microbiol.* **57**, 2440–2443 (1991).
45. B. Palenik, O. C. Zafiriou, F. M. M. Morel, Hydrogen peroxide production by a marine phytoplankter1. *Limnol. Oceanogr.* **32**, 1365–1369 (1987).
46. E. Lee-Ruff, The organic chemistry of superoxide. *Chem. Soc. Rev.* **6**, 195–214 (1977).
47. J. M. Burns *et al*., Methods for reactive oxygen species (ROS) detection in aqueous environments. *Aquat. Sci.* **74**, 683–734 (2012).
48. G. C. Kettler *et al*., Patterns and implications of gene gain and loss in the evolution of Prochlorococcus. *PLoS Genet.* **3**, e231 (2007).
49. R. G. Petasne, R. G. Zika, Fate of superoxide in coastal sea water. *Nature* **325**, 516–518 (1987).
50. S. S. Andrews, S. Caron, O. C. Zafiriou, Photochemical oxygen consumption in marine waters: A major sink for colored dissolved organic matter? *Limnol. Oceanogr.* **45**, 267–277 (2000).

51. K. Wuttig, M. I. Heller, P. L. Croot, Pathways of superoxide (O2(-)) decay in the Eastern Tropical North Atlantic. *Environ. Sci. Technol.* **47**, 10249–10256 (2013).
52. M. I. Heller, P. L. Croot, Superoxide decay kinetics in the southern ocean. *Environ. Sci. Technol.* **44**, 191–196 (2010).
53. J. W. Moffett, O. C. Zafiriou, An investigation ofhydrogen peroxide chemistry in surface waters of Vineyard Sound with H218O2 and 18O2. *Limnol. Oceanogr.* **35**, 1221–1229 (1990).
54. M. J. Hopwood, I. Rapp, C. Schlosser, E. P. Achterberg, Hydrogen peroxide in deep waters from the Mediterranean Sea, South Atlantic and South Pacific Oceans. *Sci. Rep.* **7**, 43436 (2017).
55. L. C. Powers, L. C. Babcock-adams, J. K. Enright, W. L. Miller, Probing the photochemical reactivity of deep ocean refractory carbon (DORC): Lessons from hydrogen peroxide and superoxide kinetics. *Mar. Chem.* **177**, 306–317 (2015).
56. L. C. Powers, W. L. Miller, Apparent quantum efficiency spectra for superoxide photoproduction and its formation of hydrogen peroxide in natural waters. *Front. Mar. Sci.* **3**, 235 (2016).
57. Y. Zhang, N. V. Blough, Photoproduction of one-electron reducing intermediates by chromophoric dissolved organic matter (CDOM): Relation to O2– and H2O2 photoproduction and CDOM photooxidation. *Environ. Sci. Technol.* **50**, 11008–11015 (2016).
58. L. C. Powers, W. L. Miller, Hydrogen peroxide and superoxide photoproduction in diverse marine waters: A simple proxy for estimating direct CO_2 photochemical fluxes. *Geophys. Res. Lett.* **42**, 7696–7704 (2015).
59. A. Regaudie-de-Gioux, S. Lasternas, S. Agustí, C. M. Duarte, Comparing marine primary production estimates through different methods and development of conversion equations. *Front. Mar. Sci.* **1**, 19 (2014).
60. J. H. Martin, G. A. Knauer, D. M. Karl, W. W. Broenkow, Vertex–carbon cycling in the northeast pacific. *Deep Res. Part a-Oceanogr. Res. Pap.* **34**, 267–285 (1987).
61. A. C. Redfield, B. H. Ketchum, F. A. Richards, "The influence of organisms on the composition of seawater" in *The Composition of Sea Water: Comparative and Descriptive Oceanography*, M. N. Hill, Ed. (Interscience Publishers, 1963), vol. 2, pp. 26–77.
62. L. A. Anderson, J. L. Sarmiento, Redfield ratios of remineralization determined by nutrient data analysis. *Global Biogeochem. Cycles* **8**, 65–80 (1994).

Supporting Information Appendix
for:

Dark Biological Superoxide Production as a Significant Flux and Sink of Marine Dissolved Oxygen

K.M. Sutherland, S.D. Wankel, and C.M. Hansel

www.pnas.org/cgi/doi/10.1073/pnas.1912313117

Cell Specific Superoxide Production Rate

Cell specific superoxide production rates were compiled from the scientific literature (Kustka et al. 2005; Rose et al. 2008; Diaz et al. 2013; Hansel et al. 2016; Schneider et al. 2016; Zhang et al. 2016; Plummer et al. 2019; Sutherland et al. 2019). Figure S1 displays estimates for the mean and standard error (bootstrapping, N=10,000) of each microbial extracellular superoxide production rate, with the exception of diatoms. Diatoms were calculated using the cell surface area as discussed below. The (*) in the figure below indicates alternate units of amol/μm^2/hr. While some microbial groups data sets contain non-ideal data richness for bootstrapping, we do not rely on these estimated sample parameters alone to support our conclusion. We present these estimates as one of two lines of evidence for our superoxide flux estimate, the second being field depth profiles.

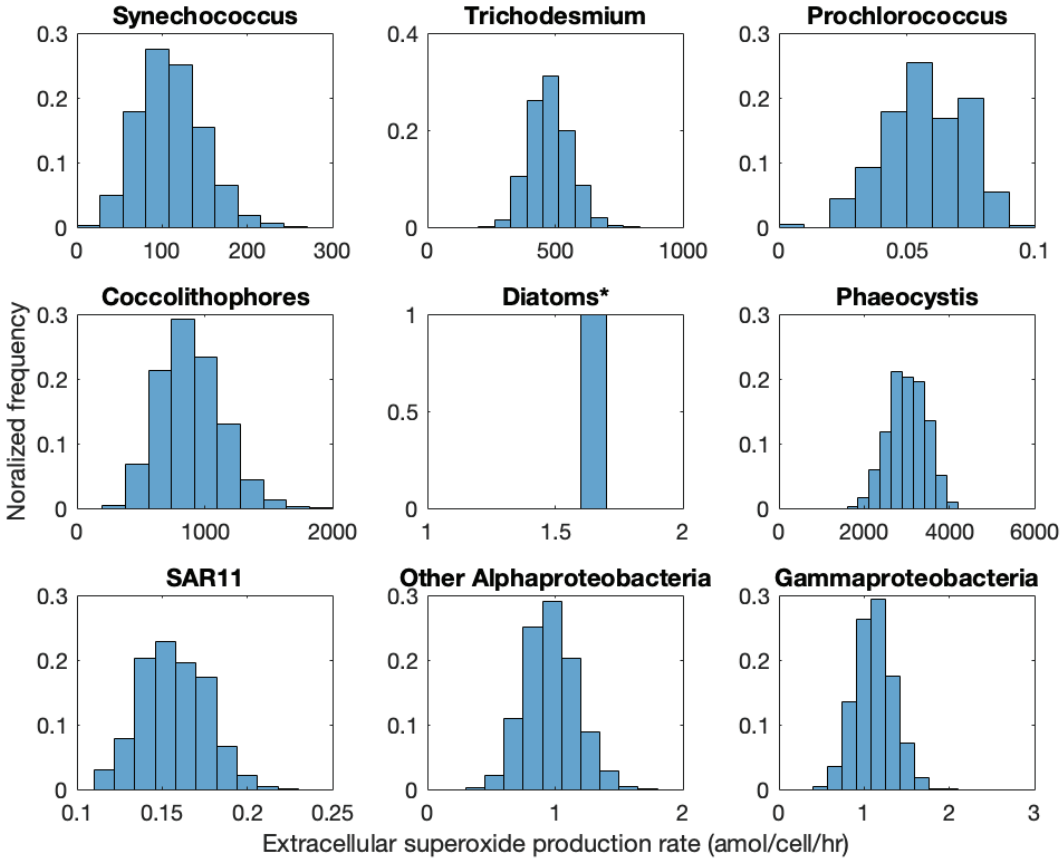

Figure S1- Distribution of mean extracellular superoxide production rates based on bootstrap estimation. The units of the mean diatom rate are amol/um^2/hr, and a more detailed treatment of diatom extracellular superoxide production estimate is provided below.

Average cell oxygen utilization rate in the global ocean

This estimate was made using a central estimate for marine net primary productivity (NPP) in Field et al. (1998) of 48.5 Pg C $year^{-1}$, gross oxygen production to carbon assimilation (GOP:NPP) value of 2.7 from Marra (2002), an estimate for the total number of prokaryotic cells in the water column from Whitman et al. (1998) (Field et al. 1998; Whitman et al. 1998; Marra 2002).

$$\frac{48.5\ Pg\ C}{year} \times \frac{1\ x\ 10^{15}\ g}{1\ Pg} \times \frac{1mol}{12.01g} \times \frac{2.7\ mol\ GOP\ (O_2)}{1\ mol\ NPP\ (C)} \times \frac{1}{1.01\ x\ 10^{29} cells} \times \frac{1\ year}{8760\ hr}$$
$$= 1.23\ x\ 10^{-17}\ \frac{mol}{cell\ hr} = 12.3\ \frac{amol}{cell\ hr}$$

Note that the product of the first four terms in the above equation gives marine gross oxygen production of 1.09×10^{16} mol O_2 year^{-1}.

Cell Number Estimates

The estimates of cell count, net primary production, and cell size have an unknown degree of uncertainty and likely contain bias toward well-studied regions and microbial groups. To account for this uncertainty in our estimation of the mean extracellular superoxide flux in the ocean, we let the cell counts for each biological grouping vary ±30% (uniform distribution) about the cell count estimates that we describe below.

Cell number estimates for each marine group were either obtained directly from previous estimates or calculated from parameters in relevant scientific literature. Estimates of *Alphaproteobacteria* and *Gammaproteobacteria* were made by multiplying estimates of total bacteria in the water column (1.01×10^{29} cells) (Whitman et al. 1998) by relative abundances of each group in the water column (43% and 27%, respectively) (Zinger et al. 2011). The *Pelagibacterales* cell number was taken directly from a previous estimate (Giovannoni 2017): 2.4×10^{28} cells. Cell numbers for *Prochlorococcus* and *Synechococcus* were taken from annual mean global abundance estimates: 2.9×10^{27} cells and 7.0×10^{26}, respectively (Flombaum et al. 2013). The data used to estimate diatom abundance was taken from a global diatom database (Leblanc et al. 2012); a cell estimate of 2.6×10^{24} diatoms was made using the annual diatom biomass (as carbon) production and the mean carbon content of each diatom cell (see diatom section below). The biomass of *Trichodesmium* in the global ocean is estimated using biomass distributions available in the Community Earth Systems Model (CESM) Large Ensemble Project using the following file (Kay et al. 2015): b.e11.B20TRC5CNBDRD.f09_g16.001.pop.h.diazC.185001-200512. This contains the distribution of carbon from diazotrophs. For simplicity, we assigned each spatial cell in the model the average carbon content over the ten-year period from January 1995 to December 2005. *Trichodesmium* cell numbers were derived using the annual average diazotroph biomass from CESM and *Trichodesmium* cell carbon content (Goebel et al. 2008) (42 pg C cell^{-1}), producing a total of 4.6×10^{23} cells. Similarly, *Phaeocystis* cell numbers were calculated using net *Phaeocystis* primary production (*Phaeocystis* represents 13% of Southern ocean net primary production, 4.5 PgC, which yields 0.58 PgC for *Phaeocystis* NPP) (Arrigo et al. 2008; Wang and Moore 2011; Rousseaux and Gregg 2014) and a mean *Phaeocystis* cell size (15 pg C cell^{-1}) (Schoemann et al. 2005; Vogt et al. 2012), producing an annual *Phaeocystis* cell count of 3.9×10^{25} cells. *Coccolithophore* cell counts were determined using the fraction of primary production attributed to the clade (21%) (Rousseaux and Gregg 2014) times global marine NPP (48.5 Pg C year^{-1}) (Field et al. 1998) and the mean *Coccolithophore* cell biomass (weighted average of each species from O'brien et al. 2013, 39.3 pg C/cell) (O'Brien et al. 2013) producing a total cell count of 2.6×10^{26} cells.

Diatom extracellular superoxide production

The diatom cell normalized extracellular $O_2^{\bullet-}$ is much less straightforward to estimate than other phytoplankton groups, as the classification division of diatoms is coarser than for the other clades

discussed in this study. The biovolume of diatoms span up to 9 orders of magnitude, requiring discrete accounting for cell size in assigning this group a cell specific superoxide production rate (Leblanc et al. 2012). Table S1 shows the surface area normalized extracellular superoxide production rates for the diatoms included in this study.

Table S1

Organism	Superoxide production rate (amol cell^{-1} hr^{-1})	Source of rate	Surface area normalized rate (amol cell^{-1} μm^{-2} hr^{-1})	Source of surface area estimate
Coscinodiscus	900-13,400	Hansel et al. 2016 (Hansel et al. 2016)	0.18, 0.29	Hansel et al. 2016 (Hansel et al. 2016)
Thalassiosira oceananica	60	Schneider et al. 2016 (Schneider et al. 2016)	0.77	Maldonado et al. 2001 (Maldonado and Price 2001)
Thalassiosira pseudonana	75	Schneider et al. 2016 (Schneider et al. 2016)	1.47	Rose et al. 2008 (Rose et al. 2008)
Thalassiosira pseudonana (Low Fe)	830	Rose et al. 2008 (Rose et al. 2008)	16.27	Rose et al. 2008 (Rose et al. 2008)
Thalassiosira pseudonana (High Fe)	450	Rose et al. 2008 (Rose et al. 2008)	8.82	Rose et al. 2008 (Rose et al. 2008)
Thalassiosira weissflogii	840	Kustka et al. 2005 (Kustka et al. 2005)	1.83	Rose et al. 2008 (Rose et al. 2008)
Thalassiosira weissflogii	252	Schneider et al. 2016 (Schneider et al. 2016)	0.55	Rose et al. 2008 (Rose et al. 2008)
Thalassiosira weissflogii (Low Fe)	1,300	Rose et al. 2008 (Rose et al. 2008)	2.83	Rose et al. 2008 (Rose et al. 2008)
Thalassiosira weissflogii (High Fe)	800	Rose et al. 2008 (Rose et al. 2008)	1.74	Rose et al. 2008 (Rose et al. 2008)

The range of extracellular superoxide production rates falls within a much narrower range when normalized to cell surface area, as shown in the table. For this reason, we estimated the total extracellular superoxide production from diatoms using the median surface area normalized production rate listed above (1.6 amol cell^{-1} μm^{-2} hr^{-1}). To determine the cell abundances and their relative contribution to the marine superoxide flux, we turned to a diatom database containing >200,000 georeferenced diatom observations that include estimates of biomass, biovolume, and surface area (Leblanc et al. 2012). None of these cell parameters can be approximated as a normal distribution. The cell surface area and biomass all have considerable skew (e.g. mean surface area =2.9x10^4 μm^2 vs median surface area = 4825 μm^2). Using the median cell biomass as an estimator for calculating diatom abundance will overestimate small cells, which have a higher surface area to volume ratio, and will therefore contribute more significantly to the superoxide flux. Using the mean biomass to calculate diatom abundance places significant weight on exceptionally large diatoms, but will produce a more conservative estimate of global cell count and cell surface area to volume ratio. We calculate the annual diatom cell count using the fraction of NPP contributed by diatoms (52%), a central estimate of annual NPP (48.5 PgC), the mean diatom biomass (9,794 pgC/cell), mean diatom surface area 29,632 um^2/cell. This estimate produces a mean annual diatom cell count of 2.6x10^{24} cells in the top 200 meters of the marine water column.

Estimation of global superoxide flux

Using MATLAB, we simulated the cumulative superoxide flux, or the sum of the 9 major microbial groups reviewed in this work. Each major group's contribution to the global superoxide flux was determined by randomly assigning a cell count from a uniform distribution ranging from the -30% to +30% of the cell estimates calculated above. This cell number was then randomly

assigned a superoxide production rate, with a probability distribution shown in Figure S1. The total superoxide production flux of all 9 microbial groups was summed, and the simulation repeated a total of 1 million times. The histogram of results is shown in figure S2.

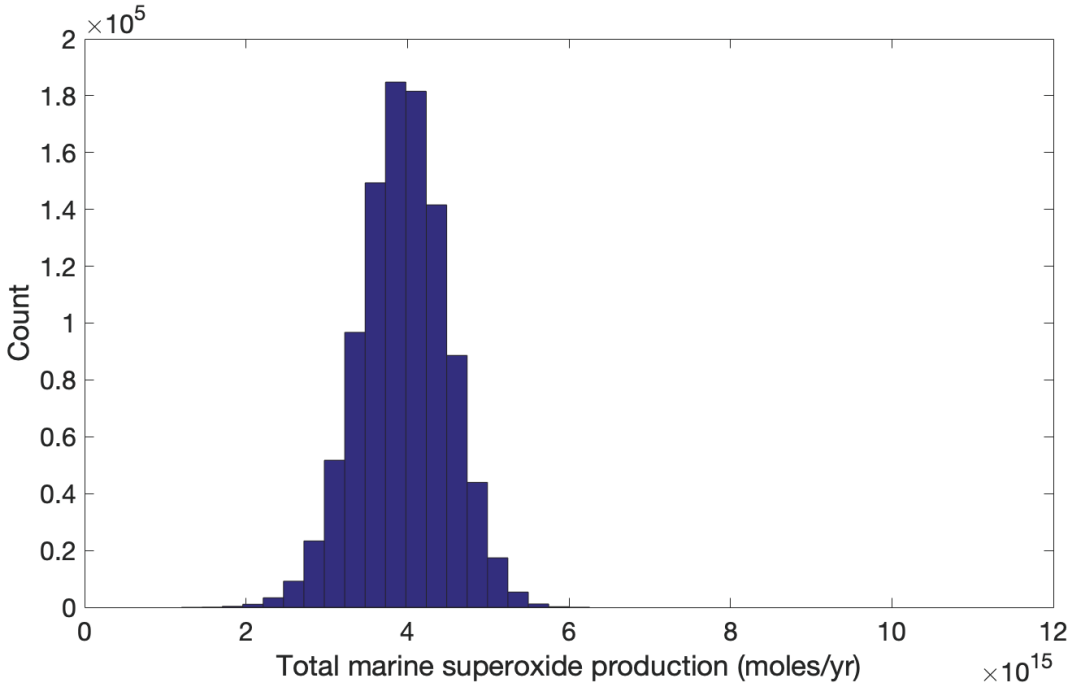

Figure S2-Histogram of the sum of extracellular superoxide production of 9 major marine microbial groups.

The 5th percentile estimate is 3.1×10^{15}, and the 95th percentile estimate is 4.8×10^{15}. The 9 microbial groups each had the following fractional contributions: diatoms: 27.2%, *Phaeocystis*: 25.3%, Coccolithophores: 19.8%, *Synechococcus*: 16.4%, *Gammaproteobacteria*: 6.5%, *Alphaproteobacter* (excluding SAR11): 3.8%, SAR11: 0.8%, *Trichodesmium*: 0.05%, *Prochlorococcus*: 0.04%.

Calculation of expected marine superoxide concentration

To test the robustness of our estimate of the global oxygen loss from extracellular superoxide production, we compare the expected superoxide concentration in the water column (based on our estimate of global production) against measurements of (dark) superoxide concentration in the water column. In order to calculate the expected superoxide concentration based on dark superoxide production, superoxide decay rates in natural water are required, which are well documented. We compiled superoxide decay rate constants from several studies on natural waters and present them in Figure S3 (Rose et al. 2008; Hansard et al. 2010; Heller and Croot 2010a; b; Heller et al. 2016; Roe et al. 2016).

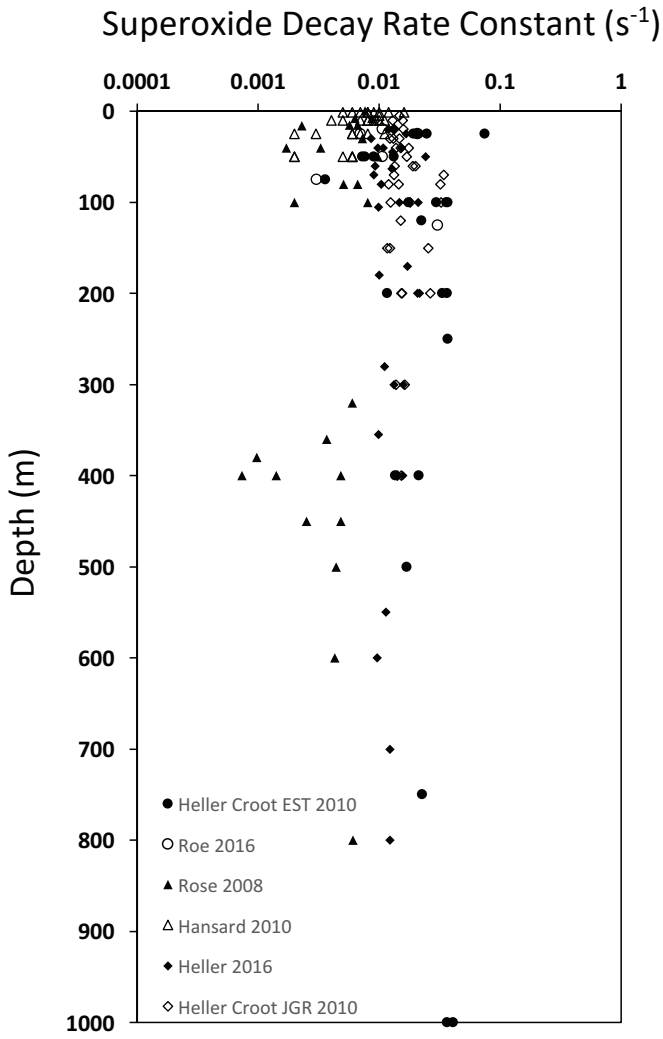

Figure S3- Compilation of superoxide decay rate constants in seawater versus seawater depth.

The complete set of decay rate constants has an approximately log-normal distribution, which was determined using one-sample Kolmogorov-Smirnov test (n=157). The mean of the natural log of all compiled superoxide decay rate constants is -4.5484 ± 0.7598 (ln(rate) ± 1 standard deviation, rate units are s^{-1}). This corresponds to a mean rate of 0.0106 s^{-1} with a 68% confidence interval ranging from 0.0050 s^{-1} to 0.0226 s^{-1}.

To calculate the expected superoxide concentration in seawater we began with an annual estimate for global superoxide flux. The total global superoxide flux was divided between the surface and the deep ocean based on estimates from Whitman et al. (1998) for the proportion of non-phototroph organisms above and below 200 meters (Whitman et al. 1998). The annual gross superoxide production was divided by the volume of water in the surface and deep ocean, respectively, yielding volume normalized annual superoxide production rates (mol L^{-1} yr^{-1}). Annual production rates were divided by the superoxide decay rate constant to determine the steady-state concentration. Given that the half-life superoxide is on the order of 1 minute or less, steady-state concentrations are achieved quickly. The following table summarizes the calculations:

Table S2

	Above 200 m	**Below 200 m**
Surface area of ocean (m^2)	$3.62x10^{14}$	$3.62x10^{14}$
Volume (m^3)	$7.24x10^{16}$	$1.34x10^{18}$
Fraction of phototroph dark superoxide production (%)	100	0
Fraction of heterotroph dark superoxide production (%)	39.5	60.5
Total superoxide produced (mol yr^{-1})	$3.68x10^{15}$	$2.67x10^{14}$
Total superoxide production rate per volume (mol yr^{-1} m^{-3})	$5.08x10^{-2}$	$1.99x10^{-4}$
Total superoxide production rate per volume (mol L^{-1} s^{-1})	$1.61x10^{-12}$	$6.31x10^{-15}$
Average concentration using k=0.0106 s-1 (pM)	152	0.6
Concentration using 1sd rate below average mean (pM)	322	1.3
Concentration using 1sd rate above average mean (pM)	71	0.3

Our estimates for global dark superoxide production predict the surface ocean will have an average concentration of 152 pM (68% confidence interval 71 to 322 pM) and the dark ocean a concentration of 0.6 pM (68% confidence interval 0.3 to 1.3 pM).

References

Arrigo, K. R., G. L. van Dijken, and S. Bushinsky. 2008. Primary production in the Southern Ocean, 1997-2006. J. Geophys. Res. **113**: 27. doi:10.1029/2007jc004551

Diaz, J. M., C. M. Hansel, B. M. Voelker, C. M. Mendes, P. F. Andeer, and T. Zhang. 2013. Widespread Production of Extracellular Superoxide by Heterotrophic Bacteria. Science (80-.). **340**: 1223–1226. doi:10.1126/science.1237331

Field, C. B., M. J. Behrenfeld, J. T. Randerson, and P. Falkowski. 1998. Primary production of the biosphere: Integrating terrestrial and oceanic components. Science (80-.). **281**: 237–240. doi:10.1126/science.281.5374.237

Flombaum, P., J. L. Gallegos, R. A. Gordillo, and others. 2013. Present and future global distributions of the marine Cyanobacteria Prochlorococcus and Synechococcus. Proc. Natl. Acad. Sci. U. S. A. **110**: 9824–9829. doi:10.1073/pnas.1307701110

Giovannoni, S. J. 2017. SAR11 Bacteria: The Most Abundant Plankton in the Oceans, p. 231–255. *In* Annual Review of Marine Science, Vol 9. Annual Reviews.

Goebel, N. L., C. A. Edwards, B. J. Carter, K. M. Achilles, and J. P. Zehr. 2008. Growth and carbon content of three different-sized diazotrophic cyanobacteria observed in the subtropical North Pacific. J. Phycol. **44**: 1212–1220. doi:10.1111/j.1529-8817.2008.00581.x

Hansard, S. P., A. W. Vermilyea, and B. M. Voelker. 2010. Deep-Sea Research I Measurements of superoxide radical concentration and decay kinetics in the Gulf of Alaska. Deep. Res. Part I **57**: 1111–1119. doi:10.1016/j.dsr.2010.05.007

Hansel, C. M., C. Buchwald, J. M. Diaz, J. E. Ossolinski, S. T. Dyhrman, B. A. S. Van Mooy, and D. Polyviou. 2016. Dynamics of extracellular superoxide production by Trichodesmium colonies from the Sargasso Sea. Limnol. Oceanogr. **61**: 1188–1200. doi:10.1002/lno.10266

Heller, M. I., and P. L. Croot. 2010a. Superoxide Decay Kinetics in the Southern Ocean. Environ. Sci. Technol. **44**: 191–196. doi:10.1021/es901766r

Heller, M. I., and P. L. Croot. 2010b. Kinetics of superoxide reactions with dissolved organic matter in tropical Atlantic surface waters near Cape Verde (TENATSO). J. Geophys. Res. **115**. doi:10.1029/2009jc006021

Heller, M. I., K. Wuttig, and P. L. Croot. 2016. Identifying the Sources and Sinks of CDOM/FDOM across the Mauritanian Shelf and Their Potential Role in the Decomposition of Superoxide (O2-). Front. Mar. Sci. **3**. doi:10.3389/fmars.2016.00132

Kay, J. E., C. Deser, A. Phillips, and others. 2015. THE COMMUNITY EARTH SYSTEM MODEL (CESM) LARGE ENSEMBLE PROJECT A Community Resource for Studying Climate Change in the Presence of Internal Climate Variability. Bull. Am. Meteorol. Soc. **96**: 1333–1349. doi:10.1175/bams-d-13-00255.1

Kustka, A. B., Y. Shaked, A. J. Milligan, D. W. King, and F. M. M. Morel. 2005. Extracellular production of superoxide by marine diatoms: Contrasting effects on iron redox chemistry and bioavailability. Limnol. Oceanogr. **50**: 1172–1180. doi:10.4319/lo.2005.50.4.1172

Leblanc, K., J. Aristegui, L. Armand, and others. 2012. A global diatom database - abundance, biovolume and biomass in the world ocean. Earth Syst. Sci. Data **4**: 149–165. doi:10.5194/essd-4-149-2012

Maldonado, M. T., and N. M. Price. 2001. Reduction and transport of organically bound iron by Thalassiosira oceanica (Bacillariophyceae). J. Phycol. **37**: 298–309. doi:10.1046/j.1529-8817.2001.037002298.x

Marra, J. 2002. Approaches to the measurement of plankton production. Phytoplankt. Product. Carbon Assim. Mar. Freshw. Ecosyst. 78–108.

O'Brien, C. J., J. A. Peloquin, M. Vogt, and others. 2013. Global marine plankton functional type biomass distributions: coccolithophores. Earth Syst. Sci. Data **5**: 259–276.

Plummer, S., A. E. Taylor, E. L. Harvey, C. M. Hansel, and J. M. Diaz. 2019. Dynamic regulation of extracellular superoxide production by the coccolithophore Emiliania huxleyi (CCMP 374). Front. Microbiol. **10**: 1546.

Roe, K. L., R. J. Schneider, C. M. Hansel, and B. M. Voelker. 2016. Measurement of dark, particle-generated superoxide and hydrogen peroxide production and decay in the subtropical and temperate North Pacific Ocean. Deep. Res. Part I-Oceanographic Res. Pap. **107**: 59–69. doi:10.1016/j.dsr.2015.10.012

Rose, A. L., E. A. Webb, T. D. Waite, and J. W. Moffett. 2008. Measurement and implications of nonphotochemically generated superoxide in the equatorial Pacific Ocean. Environ. Sci. Technol. **42**: 2387–2393. doi:10.1021/es7024609

Rousseaux, C., and W. Gregg. 2014. Interannual variation in phytoplankton primary production at a global scale. Remote Sens. **6**: 1–19.

Schneider, R. J., K. L. Roe, C. M. Hansel, and B. M. Voelker. 2016. Species-Level Variability in Extracellular Production Rates of Reactive Oxygen Species by Diatoms. Front. Chem. **4**. doi:10.3389/fchem.2016.00005

Schoemann, V., S. Becquevort, J. Stefels, W. Rousseau, C. Lancelot, V. Rousseau, and C. Lancelot. 2005. Phaeocystis blooms in the global ocean and their controlling mechanisms: a review. J. Sea Res. **53**: 43–66. doi:10.1016/j.seares.2004.01.008

Sutherland, K. M., A. Coe, R. J. Gast, and others. 2019. Extracellular superoxide production by key microbes in the global ocean. Limnol. Oceanogr.

Vogt, M., C. O'Brien, J. Peloquin, and others. 2012. Global marine plankton functional type biomass distributions: *Phaeocystis* spp. Earth Syst. Sci. Data **4**: 107–120. doi:10.5194/essd-4-107-2012

Wang, S. L., and J. K. Moore. 2011. Incorporating Phaeocystis into a Southern Ocean ecosystem model. J. Geophys. Res. **116**: 18. doi:10.1029/2009jc005817

Whitman, W. B., D. C. Coleman, and W. J. Wiebe. 1998. Prokaryotes: The unseen majority. Proc. Natl. Acad. Sci. U. S. A. **95**: 6578–6583. doi:10.1073/pnas.95.12.6578

Zhang, T., C. M. Hansel, B. M. Voelker, and C. H. Lamborg. 2016. Extensive Dark Biological Production of Reactive Oxygen Species in Brackish and Freshwater Ponds. Environ. Sci. Technol. **50**: 2983–2993. doi:10.1021/acs.est.5b03906

Zinger, L., L. A. Amaral-Zettler, J. A. Fuhrman, and others. 2011. Global Patterns of Bacterial Beta-Diversity in Seafloor and Seawater Ecosystems. PLoS One **6**. doi:10.1371/journal.pone.0024570